Investigation of a short-wavelength laser plasma of a gas-liner pinch discharge

S. H. Glenzer,* Th. Wrubel, and H.-J. Kunze
Institut für Experimentalphysik V, Ruhr-Universität, 44780 Bochum, Federal Republic of Germany

L. Godbert-Mouret
P2IM Case 232, Centre St. Jerome Université de Provence, 13397 Marseille Cedex 20, France
(Received 9 July 1996)

We studied the axial homogeneity of a gas-liner pinch plasma where amplification of line radiation at short wavelengths had been reported in an earlier study. For this purpose we measured temporally and axially resolved the Stark-broadened $n=5$ to $n=4$ transitions in F VII. From the linewidth electron densities are deduced employing spectral line shape calculations which are tested by Thomson scattering. We observe significant plasma inhomogeneities produced by Rayleigh-Taylor instabilities. Density gradients of $\delta n_e/n_e \approx 3$ along the plasma axis on a scale length of $z<1$ mm were found. They arise when compressing large amounts of a heavy gas (fluorine) of 5–10 % total gas density in the discharge with a hydrogen pusher for short-wavelength laser studies. Reducing their amount to about 1% of the total gas density results in homogeneous discharges. In this case no amplification can be observed. [S1063-651X(97)09801-2]

PACS number(s): 52.25.Qt, 42.55.Lt, 32.30.Rj, 52.70.Kz

I. INTRODUCTION

Since the first demonstrations of amplified spontaneous emission in the soft x-ray spectral range [1,2] using large high-power lasers to produce thin, several centimeters long plasmas as a gain medium, axial discharge plasmas have been investigated to achieve similar success in the corresponding wavelength range. They have the advantage of a significantly higher efficiency for the production of high-density plasmas. Thus, this fact could allow a similar energy output of a small discharge-pumped short-wavelength laser as at present routinely obtained with large laser facilities [3,4]. For that reason, discharge-pumped plasmas are of great interest to advance a table-top size x-ray laser for laboratory applications.

In most of the investigations of discharge plasmas, however, axial nonuniformities and a disadvantageous aspect ratio of the gain medium yield to difficulties [5]. These effects limit the length of the active amplifying plasma and increase the population density of the lower laser level by radiative transport, respectively, and inhibit large gain. For these reasons there are only a few successful experiments resulting in a population inversion of excited levels which are of interest for short-wavelength lasers [6,7] or in amplification of line radiation with wavelengths smaller than 120 nm [8–13]. In particular, capillary discharges have been successful [9,11,12] over the last years where a favorable aspect ratio of the discharge is enforced by the capillary walls. Indeed a gain-length product as large as $g\ell=28$ was recently obtained for a collisionally excited $3s$-$3p$ transition in Ar IX [11,14,15]. While the argon capillary plasmas are assumed to be homogeneous, in recent investigations a possible population inversion produced by charge exchange in inhomogeneous axial discharge plasmas were considered [16,17]. However, model calculations (e.g., Ref. [16]) performed for capillary discharges could not be verified, because capillaries are hardly accessible. A measurement of spatially and temporally resolved plasma parameters is almost impossible.

In the present study we have investigated the homogeneity of a gas-liner pinch plasma performing temporally and spatially resolved measurements of the electron density. In particular, we studied plasma conditions where amplified spontaneous emission of the $4f$-$3d$ transition in O VI at $\lambda=52.1$ nm and in F VII at $\lambda=38.2$ nm was observed previously [10,18]. In case of O VI a gain-length product of $g\ell=4.5$ was observed in axial direction. Also, the radial emission showed small amplification with $g\ell=1.6$. While in case of F VII no axial emission could be detected, in radial direction amplification as large as $g\ell=3.5$ was found. For this transition three-body recombination is assumed to be the dominant population mechanism yielding to a population inversion and gain [19]. A dense narrow plasma channel which cools rapidly is required by this inversion scheme and might occur in the present experiment when the plasma converges first on axis.

Temporally and axially resolved measurements of the radial emission of the $4f$-$3d$ transition in F VII showed that radial amplification occurs only shortly before maximum pinch compression and in small regions along the height of the plasma column. Furthermore, modulations in the radial dimension of the plasma column were observed with temporally resolved two-dimensional plasma pinhole images. Since these nonuniformities develop during the compression phase of the plasma, these observations can be explained by the occurrence of Rayleigh-Taylor instabilities [10]. Hence, for a detailed comparison of the measured gain with a collisional-radiative model, the spatially resolved measurement of the electron density along the height of the plasma is most important. The electron density is critical for the determination of the number density of ionic emitters and of electron-collisional equilibration of excited ionic states. In plasma regions with electron densities that are too low, too few emit-

*Present address: L-399, Lawrence Livermore National Laboratory, P.O. Box 808, Livermore, California 94551.

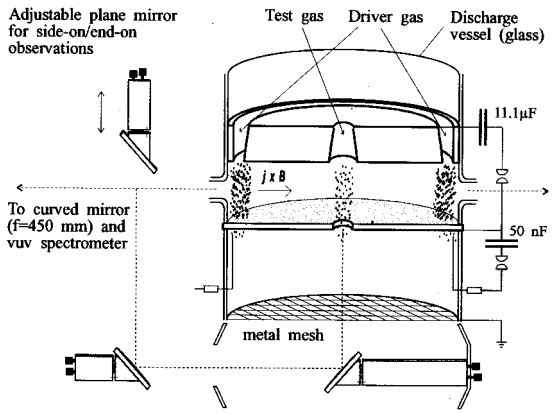

FIG. 1. Schematic of the gas-liner pinch.

ters are present which participate in the amplification process. In regions with electron densities that are too high, a possible population inversion is equilibrated within short time scales due to electron collisions. Both cases result in low gain.

For these reasons we measured temporally and spatially resolved the electron density with the Stark broadened $n=5$ to $n=4$ transitions in F VII. In a first series of experiments we produced homogeneous plasma conditions and verified spectral line broadening calculations according to Refs. [20,21]. This was achieved by measuring simultaneously the spectral line shape of the $n=5$ to $n=4$ transitions in F VII and 90° Thomson scattering spectra from the midplane of the discharge.

In a second series of experiments we measured the $n=5$ to $n=4$ transitions in F VII for plasma conditions where amplification of the $4f$-$3d$ transition in F VII has been observed. We find dense spots with $n_e \approx 7\times10^{18}$ cm^{-3} along the axis with $z=1$ mm height, giving rise to significant density gradients of $\delta n_e/n_e \approx 3$ on small scales of $z<1$ mm. This result is the first quantitative measurement of a density gradient in an axial discharge. Our findings are of importance to the understanding of the formation and radiation of z-pinch plasmas [22], where only very recently quantitative measurements [23] and simulations [24] of hot and dense spots have been performed.

II. EXPERIMENT

A. Plasma source

We used a gas-liner pinch discharge as plasma source as described earlier [10,25–27]. It resembles a z pinch with a special gas inlet system (Fig. 1). By means of a fast electromagnetic valve, the so-called driver gas (hydrogen) is injected into the vacuum chamber through an annular nozzle. The diameter of the vacuum chamber is 18 cm and the electrode separation is 5 cm. Initially, the gas forms a hollow gas cylinder near the wall. It is preionized by discharging a 50-nF capacitor (20 kV) through 50 needles that are mounted underneath the lower cathode on an annulus. Discharging the main capacitor (capacitance 11.1 μF, voltage 35 kV) compresses the gas on the axis. It serves as a light pusher to compress a heavy gas (the so-called test gas). The latter is injected independently along the axis of the discharge chamber by a second fast electromagnetic valve through a nozzle in the center of the upper electrode. It is dissociated and ionized by the imploding driver gas and by ohmic heating resulting in a plasma column of 1–2 cm diameter and 5 cm length.

For the present investigation the test gas was a mixture of 10% SF_6 in hydrogen. Relatively low densities of the heavy test gas in the discharge center of the order of 1% of the driver gas density give a radially and axially homogeneous discharge. This was shown in Refs. [28,29]. Amplification, however, was only observed when using a fairly large amount of test gas [10], i.e., 10–20 % of the driver gas density. Typical electron densities and temperatures reached in the center of the plasma column were $1\times10^{18}<n_e<6\times10^{18}$ cm^{-3} and $7.5<k_BT_e<45$ eV. The compression velocity was measured with Thomson scattering and was $(2–3)\times10^7$ cm/s. It results in a compression time of about 1 μs, as also observed with a Rogowski coil. The lifetime of the plasma depends on the discharge condition and was for the present work about 0.3 μs.

Approximately 50–100 ns before maximum pinch compression we observed the largest gain. At this time the concentration of multiply ionized test gas ions in the plasma was 10% of the electron density, as determined with Thomson scattering. Using that high test gas densities results in plasma instabilities, most probably Rayleigh-Taylor instabilities. They were clearly seen in pinhole pictures of the compressing plasma column [10,30]. Their effect on the plasma conditions is investigated below.

B. Plasma spectroscopy

The plasma is accessible through four ports in the midplane of the discharge tube and through a hole in the center of the lower cathode for side-on and end-on observations, respectively. In this investigation we measured the side-on emission of F VII. For measurements in the vacuum ultraviolet (vuv) spectral range, the plasma column was imaged onto the entrance slit of a 1-m spectrometer (McPherson model 225 with a 1200 lines/mm grating blazed at 120 nm) with a 1:4 demagnification using a curved MgF_2 mirror. The slit height and width was 2 mm and 50 μm, respectively. In the exit plane of the spectrometer a microchannelplate (MCP) of Chevron type with CsI coating on the input side and a P20 phosphor at the exit side (Galileo model CEMA 3025) was mounted. We chose a gating time of the MCP of 20 ns. The output of the phosphor was further imaged on an optical multichannel analyzer (OMA, EG&G model 1456B-990G) system or a charge coupled device camera (CCD, SI model ICCD 576 G/RB). For this detection system the apparatus function was a Lorentzian with a full width at half maximum (FWHM) of 0.16 nm. By recording hydrogen continuum radiation without injection of test gas we ensured that the detection system in the vuv has equal sensitivity over the small-wavelength ranges of the unresolved $n=5$ to $n=4$ transitions at 82.5 nm, i.e., the allowed $5g$-$4f$, $5f$-$4d$, and $5d$-$4f$ and of the forbidden $5f$-$4f$, $5d$-$4d$, and $5g$-$4d$ transitions, and of the $4f$-$3d$ and $4d$-$3p$ transitions at 38.1 and 36.8 nm of F VII. These measurements also confirm that there was no unwanted impurity radiation from residual gas in the discharge tube affecting the spectrum in the investigated

wavelength interval. The spatial resolution of the detector along the axis of the discharge was about 0.3 mm.

For the detection of Thomson scattering spectra and for measurements of the $3s$-$3p$ transitions of F VII in the visible spectral range, we imaged the center of the plasma with 1:1 magnification on the entrance slit of a 1-m spectrometer (Spex model 1704 with a 1,200 lines/mm grating blazed at 1,000 nm). The slit height and width were chosen to be 2 mm and 50 μm. The spectrometer was equipped with an OMA system. The gating time was 35 ns for spectroscopic measurements and 100 ns for Thomson scattering. In the latter case the pulse length of the probe laser determines the temporal resolution of the measurements which is about 30 ns. The sensitivity of the detection system in the visible spectral range was measured by a tungsten lamp. The wavelength calibration of the detection system was carried out by employing Fe and Al hollow cathode lamps. Furthermore, their spectra provided the apparatus profile which is given by a Voigt function with 0.0071 nm Lorentzian FWHM and 0.0049 nm Gaussian FWHM.

C. Thomson scattering

We utilized 90° Thomson scattering to independently diagnose the plasma [30–32]. For this purpose we focused a ruby laser (2 J with a pulse width of 25–35 ns FWHM) into the center of the plasma column. This setup allows an independent measurement of the plasma parameters in the midplane of the plasma simultaneously with spectroscopic measurements. The analysis of the ion feature of the Thomson scattering spectra yields the proton, electron, and test gas ion temperature when fitting the theoretical form factor of Ref. [33] to the experimental scattering data by a least-squares procedure. We find the same value for the ion, electron, and test gas ion temperature. Electron densities are determined by absolutely calibrating the detection system with Rayleigh scattering on propane and using the fitted (frequency-dependent) form factor to obtain the frequency-integrated form factor by numerical integration. For small test gas (impurity) concentrations as used for the line shape measurements, deviations of this procedure from conventional methods using the Salpeter approximation to determine the frequency-integrated form factor are small [30]. Estimating the mean charge number of the test gas ions from spectroscopic measurements allowed us to determine the test gas ion concentration from the relative intensity of the so-called impurity peak of the scattering spectrum. In this way the concentration of fluorine ions is estimated to be about 1% of the electron density for the line shape measurements and 10% for the amplification studies.

III. EXPERIMENTAL RESULTS AND DISCUSSION

A. Small test gas concentrations

For the investigation of spectral line shapes relatively small test gas concentrations of the order of 1% of the electron density are used. In this case the multiply ionized test gas ions are located in the center of a homogeneous plasma column. This condition was thoroughly studied in earlier investigations [29,34] with various experimental methods. We found a homogeneous electron density distribution in radial direction for radii $r<1.1$ cm. The test gas ions are concentrated in the homogeneous central region of the plasma with $r<0.8$ cm. Also, the axial homogeneity of the plasma column was demonstrated in earlier studies [29,34].

In this paper we investigate the homogeneity quantitatively with spatially and temporally resolved measurements of the emission of the $n=5$ to $n=4$ transitions in F VII. Figure 2 shows an example of a CCD measurement for small test gas concentrations detected 20 ns before maximum pinch compression. About 1 cm of the 5-cm-long plasma column was seen by the detector. The intensity distribution as well as the linewidth clearly demonstrate that the plasma column is homogeneous. Similar results were obtained during the discharge up to 100 ns after maximum pinch compression. After that the intensity of the spectral lines decreases significantly and no reliable statement can be drawn from the measurements of these lines.

The homogeneity of the plasma allows us to compare the measured line shapes with those predicted by theoretical approximations for the electron densities and temperatures measured in the center of the plasma column with Thomson scattering. Moreover, since the concentration of the test gas ions can be controlled independently from other discharge parameters, radiative transport (self-absorption) effects can be avoided for almost all transitions. A convenient method to check the absence of self-absorption of the investigated spectral lines is to measure spectral line intensities within multiplets. The $n=5$ to $n=4$ transitions were unresolved in the present study. Therefore, we verified that the intensity ratio of the $3s^2S_{1/2}$-$3p^2P^{\circ}_{3/2}$ to the $3s^2S_{1/2}$-$3p^2P^{\circ}_{1/2}$ multiplet line in F VII was 2:1. This is in agreement with the predictions of the LS-coupling approximation and indicates that the concentration of fluorine ions was sufficiently low so that radiation transport can be ignored for the $n=5$ to $n=4$ transitions.

Figure 3 shows the comparison of a measured line profile of the $n=5$ to $n=4$ transitions in F VII at $\lambda=82.5$ nm with a profile calculated independently for the measured plasma parameters. The calculations were performed for the electron density and temperature measured with Thomson scattering using the code developed in Refs. [20,21]. In earlier studies this code was tested for the $4f$-$3d$ and $4d$-$3p$ transitions in C IV and N V [35], and for the $n=5$ to $n=4$ transitions in C IV–O VI [36]. While in the latter study ion dynamic effects were important accounting for, e.g., 25% of the line width of C IV, ion dynamics is not important for the $n=5$ to $n=4$ transitions in F VII for the present plasma conditions. It becomes obvious from Fig. 3 that the calculations agree well with the experiment for the whole spectral line profile. For electron density diagnostic purposes, on the other hand, it is not convenient to compare full experimental line shapes with calculations. In Sec. III B the full width at half maximum (FWHM) of the line profiles is used for the density determination.

Figure 4 shows the experimental linewidths (FWHM) of the $n=5$ to $n=4$ transitions in F VII as a function of the electron density which is measured simultaneously for each discharge with Thomson scattering. The experimental data are compared with calculations, which take into account Doppler broadening and the apparatus profile. Good agreement between theory and experiment is obtained. The tem-

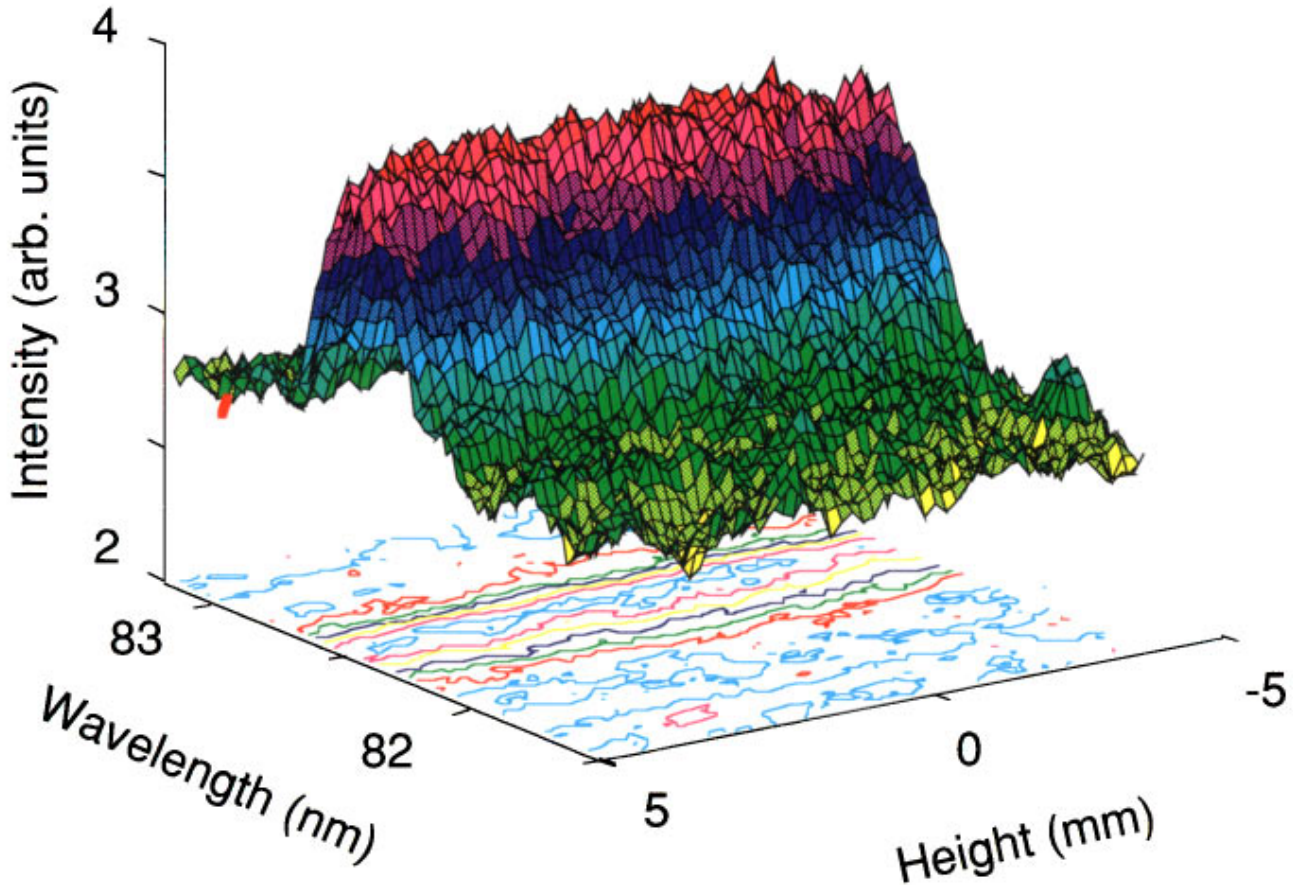

FIG. 2. Example of a CCD camera measurement of the $n=5$ to $n=4$ transitions in F VII spatially resolved along the height of the plasma column. Zero corresponds to the midplane of the discharge chamber. The experiment was performed with low test gas concentrations (1% of n_e). The intensity distribution and the linewidth show that the plasma column is homogeneous.

peratures are $10 < k_B T_e < 20$ eV. In this range our calculations show that the linewidth is not sensitive to the temperature. The uncertainty of the experimental linewidth of the individual data points is less than 10%, and the uncertainty of the electron density is 15%. However, the line width is extremely sensitive to the electron density. When deriving the electron density from the width of the spectral line, small errors in the determination of the width can result in a large error for the density. Figure 4 shows that from a single measurement, an error as large as a factor of 2 for the absolute density value can occur. On the other hand, when applying a large number of measurements the electron density of the plasma can be deduced from the line shape calcu-

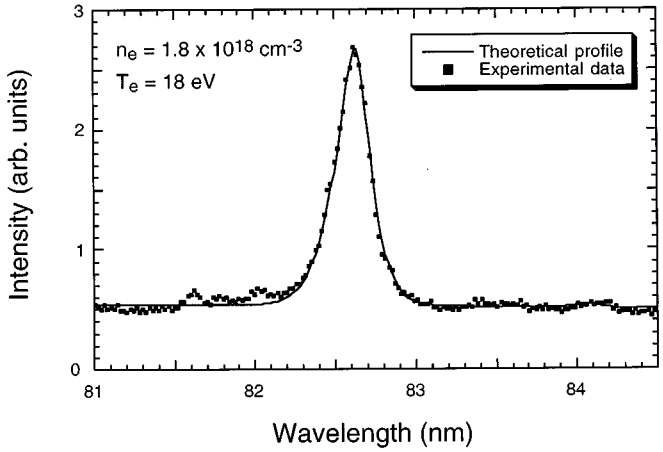

FIG. 3. Comparison of an experimental spectrum of the $n=5$ to $n=4$ transitions in F VII with theoretical calculations which are performed according to the independently measured plasma parameters from Thomson scattering.

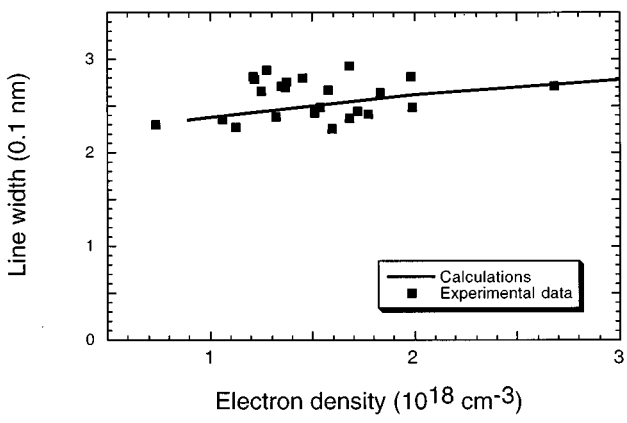

FIG. 4. Experimental Stark width (FWHM) of the $n=5$ to $n=4$ transitions in F VII and theoretical data as a function of the electron density. The calculations take into account the apparatus function as well as Doppler broadening.

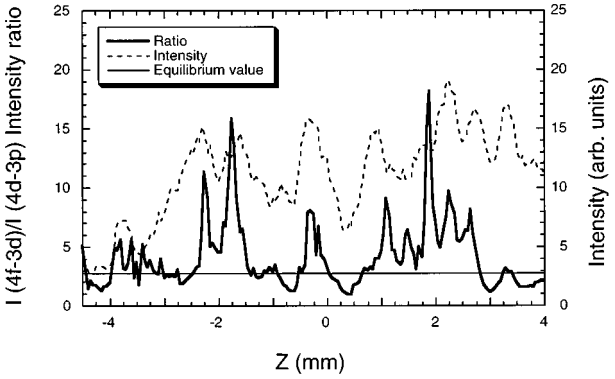

FIG. 5. Intensity ratio of the $4f$-$3d$ to the $4d$-$3p$ transition in F VII along the height of the plasma column for large amounts of test gas (10% of n_e). The measurement was performed with a CCD camera 50 ns before maximum pinch compression (—). Also shown is the equilibrium ratio of 2.8 and the intensity of the $4f$-$3d$ transition in arbitrary units ($\cdots$). The ratio is enhanced by a factor up to about 6 over the equilibrium value in small spatial regions of $z<1$ mm along the plasma axis.

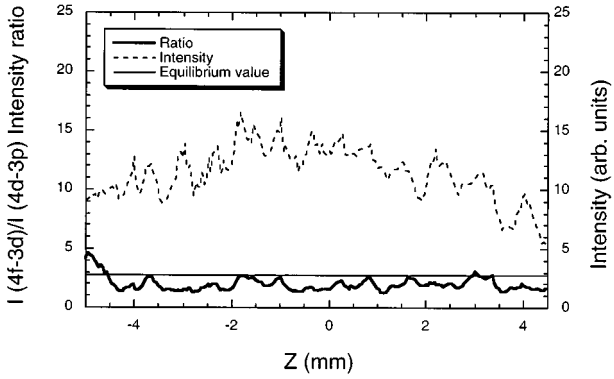

FIG. 6. Same as Fig. 5, but for smaller test gas concentrations of 5% of the electron density. The discharge is homogeneous, and the experimental intensity ratio is somewhat smaller than the equilibrium value for the whole plasma column.

lations with an uncertainty of 35%. Applying the spectral line broadening calculations to determine relative electron densities results in smaller error bars. For example, the measurement shown in Fig. 2 gives a homogeneous plasma column with a standard deviation of 15%.

B. Large test gas concentrations

Large test gas concentrations of 10–20 % of the driver gas density have been applied in a gas-liner pinch discharge for short-wavelength laser studies [10]. A population inversion and gain of the $4f$-$3d$ transition in O VI and F VII was achieved while no amplification could be found for C IV and N V. In the case of F VII we observed large amplification of the $4f$-$3d$ transition at $\lambda=38.2$ nm in the radial direction of the plasma column with $g\ell=3.5$. No axial data were obtained for this transition, because of the lack of proper multilayer mirrors.

Figure 5 shows the intensity ratio of the $4f$-$3d$ transition at $\lambda=38.2$ nm to the $4d$-$3p$ transition at $\lambda=36.8$ nm of F VII as a function of the height z of the plasma column. Large test gas concentrations were used, resulting in a fluorine ion density of 10% of the electron density. Since the upper levels $4f$ and $4d$ of both spectral lines are separated in energy by less than 400 cm^{-1} electron collisions between these levels completely dominate over all other level population mechanisms at our plasma conditions. Hence, both levels are populated according to a Boltzmann distribution [37] giving an equilibrium intensity ratio of

$$\left(\frac{I(4f-3d)}{I(4d-3p)}\right)_{eq}=2.8 \tag{1}$$

for electron temperatures above 1 eV. We verified this simplified ratio for the present plasma conditions by time-dependent collisional-radiative modeling similar to Refs. [38–40]. For these calculations, the populations of all lithiumlike levels up to $n=5$ are taken into account. Each shell with $n=6$ to $n=14$ was approximated by a single level and the population densities within these shells were approximated with a Boltzmann distribution. In addition, ground states of the He-, Be, and B-like ionization stage were included.

In Fig. 5 experimental intensity ratios as large as

$$\left(\frac{I(4f-3d)}{I(4d-3p)}\right)_{exp}=16 \tag{2}$$

are observed in small regions of about $z<1$ mm along the plasma axis. This large enhancement of the $4f$-$3d$ transition over the $4d$-$3p$ transition cannot be explained by self-absorption of the measured lines, because the optical depth of the $4f$-$3d$ spectral line is larger than that of the $4d$-$3p$ line [37], and any self-absorption effects will reduce the intensity ratio to be smaller than the equilibrium value. The measured enhancement is due to amplified spontaneous emission of the $4f$-$3d$ transition in F VII. Using the expressions of Refs. [41] to derive the gain-length product from the measured enhancement results in a maximum gain-length product of $g\ell=3.75$ for the example shown in Fig. 5.

As opposed to some measurements of $4f$-$3d$ and $4d$-$3p$ transitions in laser-produced plasmas [42] and axial discharges [13], the present investigation shows a large enhancement of the $4f$-$3d$ over the $4d$-$3p$ transition. The result of the present study is in agreement with spectra simulations of an amplifying plasma medium. They predict a factor of about three larger gain for the $4f$-$3d$ transition than for the $4d$-$3p$ transition [10,39], resulting in an increasing intensity ratio with increasing gain.

As shown in Fig. 2, a test gas concentration of about 1% of the electron density yields a homogeneous discharge. In this case no amplification can be observed. We gradually varied the test gas concentration of the plasma in the range of 1–20 % of the total gas density and observed that axial plasma inhomogeneities arise for test gas concentrations larger than 10%. For example, for a concentration of 5% almost all discharges show no gain in radial direction. This is shown in Fig. 6 where the intensity ratio of the $4f$-$3d$ to the $4d$-$3p$ transition in F VII is plotted against the height z of the plasma column. The intensity of the $4f$-$3d$ transition shows a rather homogeneous plasma condition. We find no en-

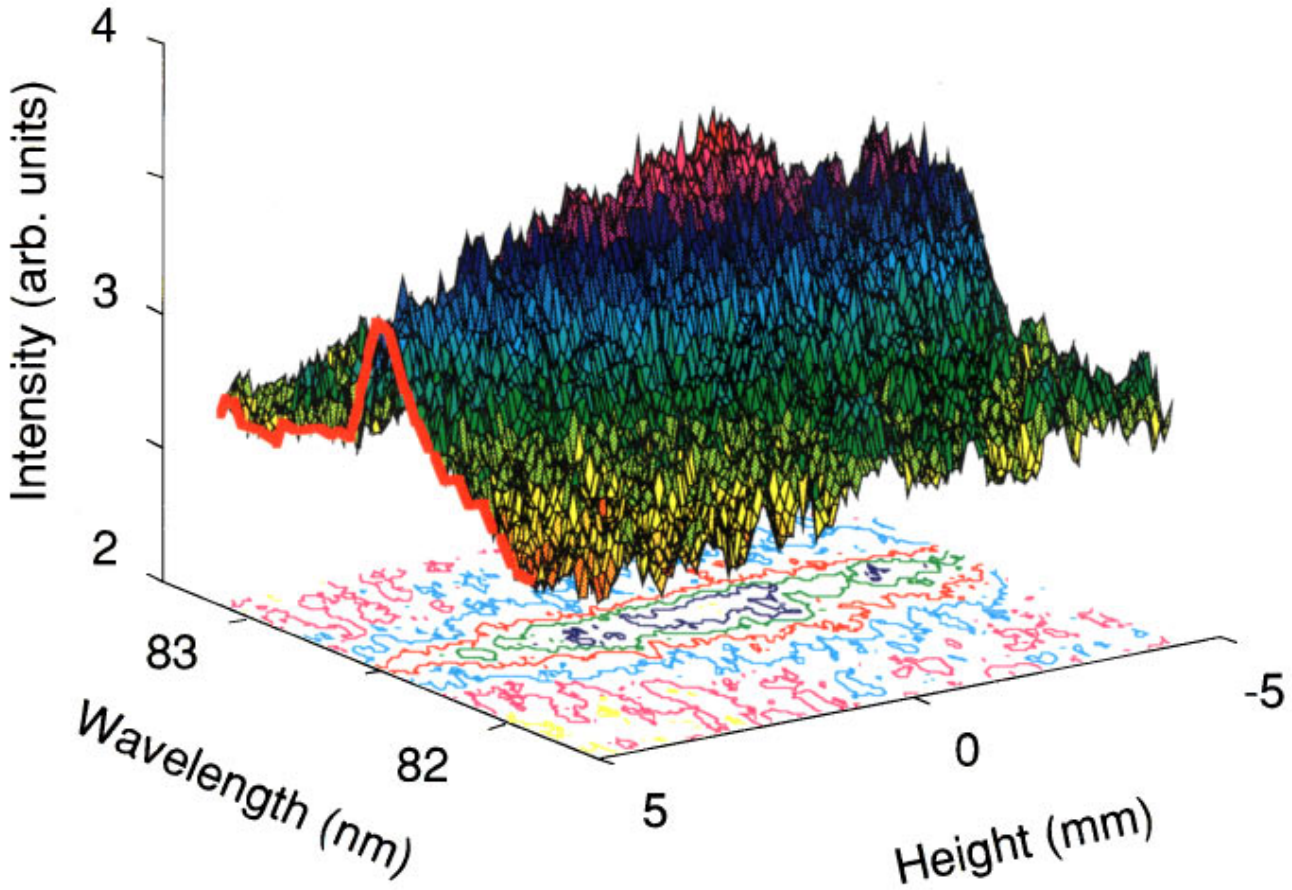

FIG. 7. Example of a CCD camera measurement of the $n=5$ to $n=4$ transition in F VII spatially resolved along the height z of the plasma column. The experiment was performed with large test gas concentrations (10% of n_e). The intensity distribution and the linewidth show significant plasma inhomogeneities along the axis.

hancement of the experimental ratio over the equilibrium value. In fact, the intensity ratio of the $4f$-$3d$ transition to the $4d$-$3p$ transition is somewhat smaller than the equilibrium value which is probably due to self-absorption.

These data demonstrate the importance of using a fairly large amount of test gas in the center of the discharge to produce a population inversion and gain of the $4f$-$3d$ transition in F VII. However, simultaneously with increasing heavy test gas densities, Rayleigh-Taylor instabilities of the compressing plasma occur giving rise to axial variations of the amplification.

The growth of magnetically driven Rayleigh-Taylor instabilities has been recently investigated for the Pegasus discharge [43]. By two-dimensional modeling the authors found that the details of the instabilities such as the large-scale features are not sensitive to the choice of the initial perturbations. Although a large number of different modes were initially present in the calculations, the largest structures which eventually break through the plasma have wavelength of the order of the thickness of the plasma itself. This computational result is in agreement with observations carried out with framing cameras [43,44]. In the present study we find similar results. The dominant features of the Rayleigh-Taylor instability are separated by about 1–2 cm along the plasma axis and are comparable with the diameter of the plasma column. This is observed with a time-resolved extreme ultraviolet pinhole camera (see Fig. 5 of Ref. [10] and Fig. 4 of Ref. [30]). However, the line emission of F VII ions is dominated by modes with smaller wavelengths which where also observable on the pinhole measurements. It can be seen in Fig. 5 that the dominant wavelength is about 1.3 mm.

On the same axial scale length, significant electron density variations occur inducing the large axial intensity and gain variations. Figure 7 shows a CCD camera measurement of the axially resolved $n=5$ to $n=4$ transitions in F VII with 10% fluorine ion density on the discharge axis. The intensity as well as the line width shows variations on scales of $z<1$ mm along the axis (Fig. 8). The linewidth (FWHM) of the $n=5$ to $n=4$ transitions in F VII assumes peak values of about 0.35 nm. Applying line broadening calculations (Refs. [20,21], Sec. III A) we find corresponding electron densities of $n_e \approx 7\times10^{18}$ cm^{-3}. The high density spots have a height of about 1 mm, and the density gradients are $\delta n_e/n_e \approx 3$ on a scale of $z<1$ mm. In addition to these small scale density peaks, a large scale inhomogeneity with a height of the order of 5 mm can be observed in Fig. 7.

It should be noted that the intensities of the spectral lines emitted from the dense spots is larger than on the average by almost a factor of 2. On the other hand, Fig. 5 shows that the highest enhancement of the $4f$-$3d$ transition over the $4d$-$3p$ transition in F VII, i.e., the highest gain, does not exactly coincide with the regions of the highest intensities of the

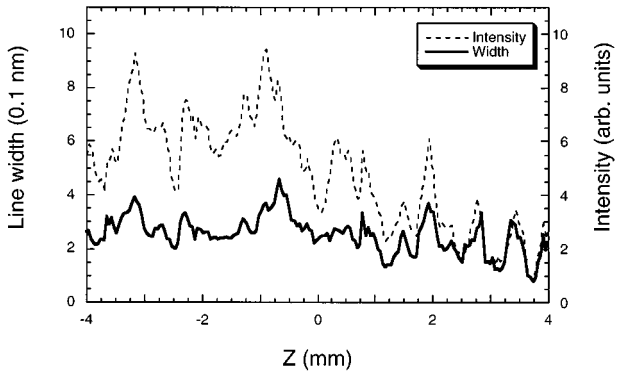

FIG. 8. Measured linewidth of the $n=5$ to $n=4$ transitions along the height of the plasma axis (—) for large test gas concentrations (10% of n_e). Also shown is the intensity of the $n=5$ to $n=4$ transitions in arbitrary units, · · · ·.

$4f$-$3d$ transitions in F VII. This observation indicates that the largest gain occurs in plasma regions of lower densities with $n_e<2\times10^{18}$ cm^{-3}. This is consistent with the results of our collisional-radiative modeling which show that a possible population inversion between the $4f$ and $3d$ levels is equilibrated in the high density regions with $n_e\approx7\times10^{18}$ cm^{-3} by electron collisions on time scales much shorter than 10 ns. For example, assuming a rapidly cooling plasma with a decay constant of 5–10 eV/ns results in a population inversion by three-body recombination of the $4f$ and $3d$ level for only a few hundred picoseconds. The temporal resolution of our measurements in the extreme ultraviolet spectral range is 20 ns. Therefore, very short laser pulses by amplified spontaneous emission processes on times scales of <1 ns could not be resolved in this study. On the other hand, in the low density regions with $n_e<2\times10^{18}$ cm^{-3} equilibration times are of the order of 10 ns, resulting in a population inversion with a duration of a few nanoseconds which is measurable with our detection system.

More detailed measurements of the electron temperature evolution of the plasma will be necessary to verify the decay constant used in the collisional-radiative modeling. These measurements will also be useful to investigate the role of charge exchange processes on the population kinetics of the plasma [16,17].

Since amplification occurs most probably in the low density regions of the plasma, the appearance of Rayleigh-Taylor instabilities and accompanying dense spots limit the length of the amplifying plasma medium in axial direction of the discharge. The Rayleigh-Taylor instabilities give rise to centimeter-size plasma features in radial direction of the plasma column. Thus, amplified spontaneous emission with a gain-length product of $g\ell=3.75$ occurs in the radial direction of the plasma column. It will be of the utmost importance to investigate the end-on emission of F VII for similar plasma conditions as achieved in this study. Although the dense spots will reduce the effective size of the amplifying medium in the axial direction and furthermore reduce the possible observable gain by absorption of the laser emission, our experimental results obtained in O VI [10] suggest that large gain of the axial $4f$-$3d$ transition in F VII can occur.

IV. SUMMARY AND OUTLOOK

We achieved a fairly large gain-length product of the $4f$-$3d$ transition in F VII at $\lambda=38.2$ nm in a plasma of the gas-liner pinch discharge. We found dense spots along the axis of the plasma and significant density gradients of $n_e/n_e\approx3$ on small scales of $z<1$ mm along the axis. They are produced by Rayleigh-Taylor instabilities of the compressing plasma column. The instabilities affect the emission of the plasma column. They give rise to plasma features of smaller than one centimeter and amplification of line radiation in the radial direction of the plasma column. For the maximum used test gas concentrations of 10–20 % of the total gas density, Rayleigh-Taylor instabilities could not be avoided limiting the length of the active medium in axial direction of the gas-liner pinch plasma. For future studies it will be most interesting to observe the axial emission of the $4f$-$3d$ transition in F VII similar to our earlier studies in O VI. The results of the present study show that the choice of the test gas concentration determines the grows of Rayleigh-Taylor instabilities in liner discharges which are of special interest for the development of a discharge-pumped short-wavelength table-top laser.

ACKNOWLEDGMENT

This research was supported by the Sonderforschungsbereich 191 of the DFG.

[1] D. L. Matthews, P. L. Hagelstein, M. D. Rosen, M. J. Eckart, N. M. Ceglio, A. U. Hazi, H. Medecki, B. J. MacCowan, J. E. Trebes, B. L. Whitten, E. M. Campbell, C. W. Hatcher, A. M. Hawryluk, R. L. Kauffman, L. D. Pleasance, G. Rambach, J. H. Scofield, G. Stone, and T. A. Weaver, Phys. Rev. Lett. **54**, 110 (1985).

[2] S. Suckewer, C. H. Skinner, H. Milchberg, C. Keane, and D. Voorhees, Phys. Rev. Lett. **55**, 1753 (1985).

[3] B. J. MacGowan, L. B. Da Silva, D. J. Fields, C. J. Keane, J. A. Koch, R. A. London, D. L. Matthews, S. Maxon, S. Mrowka, A. L. Osterheld, J. H. Scofield, G. Shimkaveg, J. E. Trebes, and R. S. Walling, Phys. Fluids B **4**, 2326 (1992).

[4] L. B. DaSilva, T. W. Barbee, Jr., R. Cauble, P. Celliers, J. Harder, H. R. Lee, R. A. London, D. L. Matthews, S. Mrowka, J. C. Moreno, D. Ress, J. E. Trebes, A. Wan, and F. Weber, Rev. Sci. Instrum. **66**, 574 (1995).

[5] J. Davis, Nav. Res. Rev. **3**, 36 (1989).

[6] J. L. Porter, R. B. Spielman, M. K. Matzen, E. J. McGuire, L. E. Ruggles, M. F. Vargas, J. P. Apruzese, R. W. Clark, and J. Davis, Phys. Rev. Lett. **68**, 796 (1992).

[7] N. Qi, D. A. Hammer, D. H. Kalantar, and K. C. Mittal, Phys. Rev. A **47**, 2253 (1993).

[8] R. W. Waynant, Phys. Rev. Lett. **28**, 553 (1972).

[9] C. Steden and H.-J. Kunze, Phys. Lett. A **151**, 534 (1990).

[10] S. Glenzer and H.-J. Kunze, Phys. Rev. E **49**, 1586 (1994).

[11] J. J. Rocca, V. Shlyaptsev, F. G. Tomasel, O. D. Cortázar, D.

Hartshorn, and J. L. A. Chilla, Phys. Rev. Lett. **73**, 2192 (1994).
[12] H.-J. Shin, D.-E. Kim, and T.-N. Lee, Phys. Rev. E **50**, 1376 (1994).
[13] T. Wagner, E. Eberl, K. Frank, W. Hartmann, D. H. H. Hoffmann, and R. Tkotz, Phys. Rev. Lett. **76**, 3124 (1996).
[14] J. J. Rocca, F. G. Tomasel, M. C. Marconi, V. N. Shlyaptsev, J. L. A. Chilla, B. T. Szapiro, and G. Giudice, Phys. Plasmas **2**, 2547 (1995).
[15] J. J. Rocca, D. P. Clark, J. L. A. Chilla, and V. N. Shlyaptsev, Phys. Rev. Lett. **77**, 1476 (1996).
[16] H.-J. Kunze, K. N. Koshelev, C. Steden, D. Uskov, and H. T. Wieschebrink, Phys. Lett. A **193**, 183 (1994).
[17] K. N. Koshelev, Yu. V. Sidelnikov, S. S. Churilov, and L. A. Dorokin, Phys. Lett. A **191**, 149 (1994).
[18] H.-J. Kunze, S. Glenzer, C. Steden, H. T. Wischebrink, K. N. Koshelev, D. Uskov, in *X-Ray Lasers 1994*, edited by C. D. Eder and D. L. Matthews, AIP Conference Proc. No. 332, (AIP, New York, 1994), pp. 380–387.
[19] L. I. Gudzenko and L. A. Shelepin, Zh. Éksp. Teor. Fiz. **45**, 1445 (1963) [Sov. Phys. JETP **18**, 998 (1964)]; R. C. Elton, *X-Ray Lasers* (Academic, New York, 1990).
[20] L. Godbert, A. Calisti, R. Stamm, B. Talin, R. W. Lee, and L. Klein, Phys. Rev. E **49**, 5644 (1994).
[21] B. Talin, A. Calisti, L. Godbert, R. Stamm, and R. W. Lee, Phys. Rev. A **51**, 1918 (1995).
[22] N. R. Pereira and J. Davis, J. Appl. Phys. **64**, R1 (1988).
[23] T. Nash, C. Deeney, M. Krishnan, R. R. Prasad, P. D. Lepell, and L. Warren, J. Quant. Spectrosc. Radiat. Transfer **44**, 485 (1990).
[24] S. Maxon, J. H. Hammer, J. L. Eddleman, M. Tabak, G. B. Zimmerman, W. E. Alley, K. G. Estabrook, J. A. Harte, T. J. Nash, T. W. L. Sanford, and J. S. De Groot, Phys. Plasmas **3**, 1737 (1996).
[25] K. H. Finken and U. Ackermann, Phys. Lett. **85A**, 278 (1981).
[26] K. H. Finken and U. Ackermann, J. Phys. D **15**, 615 (1982).
[27] H.-J. Kunze, in *Spectral Line Shapes*, edited by R. J. Exton (Deepak, Hampton, 1987), pp. 23–35.
[28] S. Glenzer, N. I. Uzelac, and H.-J. Kunze, Phys. Rev. A **45**, 8795 (1992).
[29] S. Glenzer, in *Spectral Line Shapes*, edited by A. D. May, J. R. Drummond, and E. A. Oks, AIP Conf. Proc. No. 328 (AIP, New York, 1994), pp. 134–150.
[30] T. Wrubel, S. Glenzer, S. Büscher, and H.-J. Kunze, J. Atmos. Terr. Phys. **58**, 1077 (1996).
[31] H.-J. Kunze, in *Plasma Diagnostics*, edited by W. Lochte-Holtgreven (Amsterdam, North-Holland, 1968) pp 550–616.
[32] A. Gawron, S. Maurmann, F. Böttcher, A. Meckler, and H.-J. Kunze, Phys. Rev. A **38**, 4737 (1988).
[33] D. E. Evans, Plasma Phys. **12**, 573 (1970).
[34] S. H. Glenzer, in *Atomic Processes in Plasmas*, edited by A. Osterheld and W. Goldstein, AIP Conf. Proc. No. 381 (AIP, New York, 1996), pp. 109–122.
[35] L. Godbert, A. Calisti, R. Stamm, B. Talin, S. Glenzer, H.-J. Kunze, J. Nash, R. W. Lee, and L. Klein, Phys. Rev. E **49**, 5889 (1994).
[36] S. Glenzer, Th. Wrubel, S. Büscher, H.-J. Kunze, L. Godbert, A. Calisti, R. Stamm, B. Talin, J. Nash, R. W. Lee, and L. Klein, J. Phys. B **27**, 5507 (1994).
[37] H. R. Griem, *Plasma Spectroscopy* (McGraw-Hill, New York, 1964).
[38] R. W. Lee, B. L. Whitten, and R. E. Strout, II, J. Quant. Spectrosc. Radiat. Transfer **32**, 91 (1984); R. W. Lee (private communication).
[39] A. Carillon, M. J. Edwards, M. Grande, M. J. de C. Henshaw, P. Jaeglé, G. Jamelot, M. H. Key, G. P. Kiehn, A. Klisnick, C. L. S. Lewis, D. O'Neill, G. J. Pert, S. A. Ramsden, C. M. E. Regan, S. J. Rose, R. Smith, and O. Willi, J. Phys. B. **23**, 147 (1990).
[40] A. Klisnick, A. Sureau, H. Guennou, C. Möller, and J. Virmont, Appl. Phys. B **50**, 153 (1990).
[41] G. J. Linford, E. E. Peressini, W. R. Sooy, and M. L. Spaeth, Appl. Opt. **13**, 379 (1974); R. A. London, Phys. Fluids **31**, 184 (1988).
[42] J. C. Moreno, H. R. Griem, S. Goldsmith, and J. Knauer, Phys. Rev. A **39**, 6033 (1989).
[43] D. L. Peterson, R. L. Bowers, J. H. Brownell, A. E. Greene, K. D. McLenithan, T. A. Oliphant, N. F. Roderick, and A. J. Scannapieco, Phys. Plasmas **3**, 368 (1996).
[44] K. L. Wong, P. T. Springer, H. C. Bruns, J. A. Emig, J. H. Hammer, A. L. Osterheld, and C. Deeney (unpublished).